SEIRA and SERS Effects in Cyclopentabithiophenethiol-Capped Gold Nanoparticles

DATASET *in* THE JOURNAL OF PHYSICAL CHEMISTRY C · JUNE 2010

Impact Factor: 4.77 · DOI: 10.1021/jp1027355

SEIRA and SERS Effects in Cyclopentabithiophenethiol-Capped Gold Nanoparticles

B. Vercelli and G. Zotti*

Istituto CNR per l' Energetica e le Interfasi, c.o Stati Uniti 4, 35127 Padova, Italy

A. Berlin

Istituto CNR di Scienze e Tecnologie Molecolari, via C.Golgi 19, 20133 Milano, Italy

C. Capel Ferrón, V. Hernández, and J. T. López Navarrete

Departamento de Química Física, Facultad de Ciencias. Universidad de Málaga, 29071-Málaga, Spain

Received: March 26, 2010; Revised Manuscript Received: June 11, 2010

Gold nanoparticles capped with cyclopentadithiophene via hexylsulfide bridges have undergone FTIR and Raman analysis, before and after dithiophene oxidative coupling, with the support of DFT calculations. A strong SEIRA effect has revealed an almost parallel disposition of the oligothiophene ring plane in respect to the gold surface, enhanced by polymerization. An unusual SERS enhancement of the oligothiophene ring stretching band has been assigned to coordination of the gold surface of neighboring particles via the thiophene sulfur atoms.

1. Introduction

Inorganic nanoparticles and π-conjugated polymers have unique applications in electronic and optoelectronic devices and in particular for fabrication of flexible light-emitting diodes[1] since a high surface contact with the polymeric emitter results in lower turn-on voltage and higher quantum efficiency. A light-emitting diode may have enhanced characteristics also by surface plasmon (SP) coupling with gold nanoparticles (AuNPs). Applied to, for example, indium gallium nitride quantum wells,[2] the method has a much broader range of applicability such as in organic semiconductor materials including polymers. Besides directly emitting light, electroluminescence in organic light-emitting diodes can excite surface plasmons (SPs) on the metal electrodes of the device.[3]

The SP interaction of AuNPs with the electronic excitation of oligothiophene thin films has been recently investigated.[4] The oligothiophene linker facilitates near-field coupling between adjacent nanoparticles, and disruption of the conjugation in the oligothiophene by chemical oxidation leads to a decrease in surface plasmon resonance (SPR) coupling between neighboring particles. Moreover, nanocomposites of gold nanoparticles thiol-bound to terthiophene show that the electronic systems of the terthiophene are coupled with the gold nanoparticles.[5]

SPR is also important for analytical applications such as in surface-enhanced raman scattering (SERS) and surface-enhanced infrared absorption (SEIRA). In particular SERS has been extensively studied since Van Duyne and Creighton's discovery of Raman scattering enhancement of molecules adsorbed on roughened metallic surfaces some 30 years ago.[6] Subsequent experimental and theoretical studies have attributed this observation to SPR which creates "hot" electric field spots on the curved surfaces as well as in the troughs between nanoprotrusions. Consequently, molecules that are trapped within or situated in the vicinity of these "hot" zones would experience a strong excitation field and in turn emit amplified Raman intensities. It has been amply demonstrated that surfaces consisting of closely packed but not aggregated colloidal arrays are particularly enhancing, owing primarily to the interparticle plasmon resonance.[7] The enhancement factor of SERS, estimated around 10^3 to 10^6 on roughened surfaces, is thus increased to 10^6-10^{15} using gold nanoparticles.

The literature gives several examples of oligo-(poly-)thiophene/AuNP composite materials.[8] We have recently reported the aggregation of AuNPs by pyrrole- and thiophene-based oligomers, which allowed us to produce a series of novel pyrrolethiol- and thiophenethiol-capped gold nanoparticles.[9] The thiol compounds, which form dense self-assembled monolayers on gold electrodes, react with gold nanoparticles to form monodisperse, stable, and soluble thiol-capped gold clusters which are coupled to polymeric gold clusters linked by polyconjugated bridges.

Among the used ligands, the cyclopentadithiophene thiol He_2CPDTSH (Chart 1) presents peculiar properties for the study of SP interaction with the polyconjugated chain due to the unusual perpendicular disposition of the oligothiophene axis in respect to the thiol-ended hexyl extended linear chain. For this reason, we have undertaken a vibrational (FTIR and Raman) investigation of this particular ligand and its molecular composites with gold nanoparticles, aiming in particular to detect the interaction with the SP wave of the gold nanoparticle itself.

2. Experimental Section

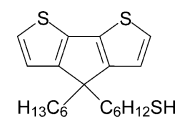

He_2CPDTSH

2.1. Chemicals and Reagents. 6-(4-Hexyl-4*H*-cyclopenta[2,1-*b*:3,4-*b*′]dithiophen-4-yl)hexane-1-thiol (He_2CPDTSH) was pre-

* To whom correspondence should be addressed. Tel: (39)049-829-5868. Fax: (39)049-829-5853. E-mail: g.zotti@ieni.cnr.it.

10.1021/jp1027355
Published on Web 07/08/2010

SCHEME 1

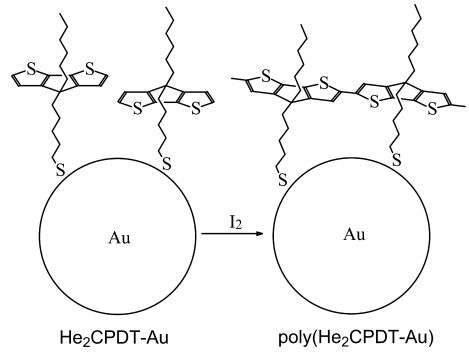

pared as described previously.[9b] Cyclopentadithiophene-capped gold nanoparticle (He_2CPDT-Au) was prepared by the ligand exchange method as reported previously.[9b] In particular, 8 mg of He_2CPDTSH (20 μmol) was added to a 10^{-2} M toluene solution of gold nanoparticles (20 mL, 200 μmol). The resulting solution was allowed to stand for 24 h at room temperature. The organic phase was then evaporated, and the residue washed subsequently with acetonitrile and EtOH (50 mL each) to produce ca. 20 mg of product (50% yield). The ligand coverage of the nanoparticles is 4×10^{-10} mol cm^{-2}.[9b]

He_2CPDT-Au nanoparticles are chemically coupled (polymerized) with iodine in $CHCl_3$ solution (see Scheme 1). In practice, 10 mg of particles dissolved in 5 mL of $CHCl_3$ is added to 4 mg of iodine in 2 mL of $CHCl_3$. The produced polymeric precipitate is filtered and dried under vacuum. The polymer is not soluble in any solvent.

2.2. Apparatus and Procedure. FTIR spectra were run on a Perkin-Elmer 2000 FTIR spectrometer. Spectra of KBr pellets were recorded on 1 mm thick samples with a 2% content of the compound. Spectra of films, cast on platinum, were recorded in reflection−absorption mode using a grazing incidence reflection unit (Specac). Spectra were recorded with 2 cm^{-1} resolution at an angle of incidence of 80° relative to the surface normal. Ten cycles were run for each spectrum, and weighted subtraction of the background at the end of the series of measurements was applied. No gas purging of the chamber was necessary. Raman spectra were recorded with a Bruker-Senterra microscope equipped with three lasers lines at 532, 633, and 785 nm and 3 cm^{-1} resolution. The power used for each laser excitation line was 0.2 mW (at 532 and 633 nm) and 10 mW (at 785 nm). Electronic spectra were run on a Perkin-Elmer Lambda 15 spectrometer.

2.3. Computational Details. Density functional theory (DFT) calculations were carried out using the Gaussian 03 program[10] running on an SGI Origin supercomputer. Becke's three-parameter exchange functional combined with the LYP correlation functional (B3LYP)[11] was employed, because it has been shown that the B3LYP functional yields geometries for medium-sized molecules similar to those obtained from the MP2 calculations with the same basis sets.[12] Moreover, the DFT force fields calculated using the B3LYP functional yield infrared spectra in very good agreement with experiments.[13] The standard 6-31G** basis set was used to obtain optimized geometries on isolated entities.[14] For the resulting ground-state optimized geometries, harmonic vibrational frequencies and infrared intensities were calculated with the B3LYP functional. Calculated frequencies were uniformly scaled down by a factor of 0.96 for the 6-31G** calculations, as recommended by Scott and Radom.[15] This scaling procedure typically has an adequate accuracy for a reliable assignment of the experimental data.

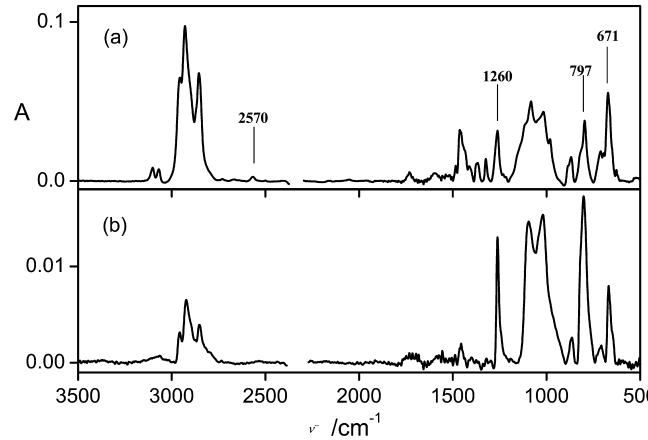

Figure 1. FTIR spectra of (a) He_2CPDTSH and (b) He_2CPDT-Au (KBr-pellets).

Thus, all vibrational frequencies reported in this work are scaled values. The theoretical spectra were obtaining by convoluting the scaled frequencies with Gaussian functions (10 cm^{-1} width at the half-height). The relative heights of the Gaussians were determined from the theoretical infrared intensities.

3. Results and Discussion

3.1. FTIR Analysis of He_2CPDTSH. The experimental FT-IR spectrum of He_2CPDTSH is displayed in Figure 1a whereas the calculated (at the B3LYP/6-31G** level) spectrum is given as Figure S1 of the Supporting Information along with the sketched eigenvectors associated with the most important bands (Figures S2 and S3 of the Supporting Information). In general, the theoretical spectra reproduce the main tendencies of the experimental features even when the absorption spectra are recorded in the solid state. In the high-energy region, the spectra show two weak bands about 3100−3070 cm^{-1} assignable to the aromatic C−H stretching modes and several well resolved peaks below 3000 cm^{-1}, corresponding to the aliphatic C−H stretching bands, all of them with a dipole derivative vector parallel to the oligothiophene rings plane. Importantly, the peak at 2570 cm^{-1} (calculated at 2567 cm^{-1}) must be assigned (see the corresponding eigenvector in the Supporting Information) to the SH stretching mode of the molecule.

The region below 1500 cm^{-1} is dominated by several normal modes at 1460, 1370, 1320, 1260, 1100−1000, 868, 797, and 671 cm^{-1}. In view of the calculated eigenvectors, the multiplets of bands at 1500−1200 cm^{-1} are due to CH_3 and CH_2 bending vibrations, and only the band at 1260 cm^{-1} (calculated at 1265 cm^{-1}) has a dipole derivative vector perpendicular to the ring plane. The broad bands at 1100−1000 cm^{-1} correspond to the C−H in-plane bendings. Finally, the C−H out-of plane bending vibrations whose wavenumbers are characteristic of the substitution position, appear in the 800−600 cm^{-1} region. We can easily identify the bands near 800 and 670 cm^{-1} as due to the C−H out-of-plane bending and, obviously, with the dipole derivative vector perpendicular to the plane of the rings.

3.2. SEIRA and FTIR Analysis of He_2CPDT-Capped Gold Nanoparticles. ***SEIRA.*** Optical properties of molecules are altered dramatically when they are adsorbed on or near some rough metal surfaces. Since its discovery, surface-enhanced infrared absorption (SEIRA) has been thoroughly investigated.[15−17] It has been proposed that the enhancement is due to a strong electromagnetic field amplified through the excitation of collective electron resonance (localized plasma oscillation) of the small metal island.[18] The infrared surface selection rule for

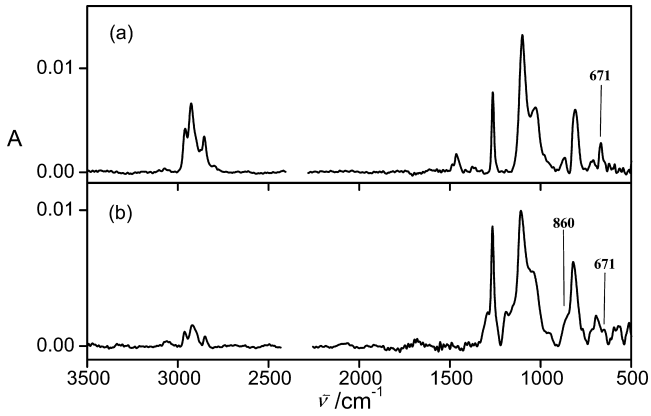

Figure 2. FTIR spectra of He_2CPDT-Au film (a) before and (b) after coupling to poly(He_2CPDT-Au).

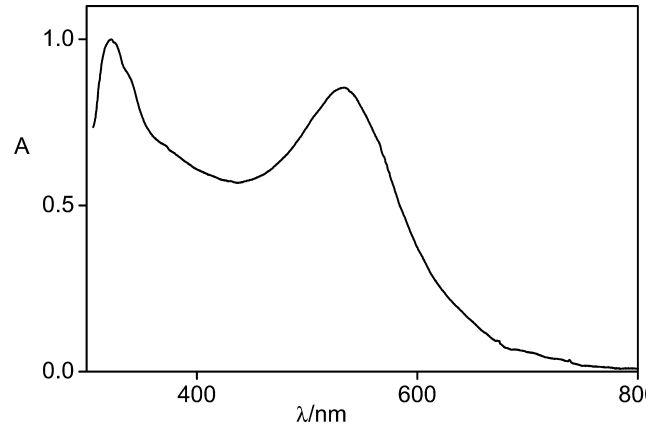

Figure 3. UV−vis spectrum of He_2CPDT-Au in toluene solution.

molecules at and near a smooth surface of an extended metal is based on the high electronic screening of all metals in the infrared spectral region. Due to the screening currents parallel to the surface within the metal, the electric vector parallel to the surface is very small compared to the perpendicular component. Therefore, the incident radiation will essentially interact with the molecular vibrations that have dipole changes oriented perpendicular to the surface. In SEIRA, molecular vibrations having transition dipole components perpendicular to the surface are selectively observed.[19]

He_2CPDT-Au Nanoparticles. The infrared spectrum of He_2CPDT-Au nanoparticles is shown in Figure 1b in comparison with the spectrum of the ligand (Figure 1a). The signals in the spectrum correspond substantially to those of free oligomer but for the significant disappearance of the weak S−H stretching, in agreement with surface immobilization via sulfide bonding. If the average molecular orientation has the oligothiophene plane parallel to the surface of the metal island, then most of its in-plane vibrations and those with the dipole derivative vector parallel to this plane will exhibit low absorptions. In contrast, out-of-plane vibrational dipoles would be parallel with the field and the corresponding modes should be enhanced in the spectrum. Taking the bands at 3100−2800 cm^{-1} (or those at 1500−1300 cm^{-1}) as typical modes with in-plane dipole derivative vector and those at 1260, 800, and 670 cm^{-1} as modes with out-of-plane derivative vector, we see in the figure that the relative intensity (2930/1260 or 2930/800) is largely decreased in the SEIRA spectrum. This good prediction indicates that the average orientation of the thiophene plane with respect to the gold surface is nearly parallel and confers a high orientation to the dithiophene-linked hexyl chain on the gold nanoparticle.

After the CPDT units in the He_2CPDT-Au nanoparticles are coupled to oligomers (sexithiophene mainly), the FTIR spectra of the film (Figure 2) indicate the appearance of a signal (as a shoulder) at 860 cm^{-1}, due to the out-of-plane γ(C−H) bending modes characteristic of 2,5-disubstituted-3-alkylthiophene and a concomitant decrease of the band at 670 cm^{-1} due to the out-of-plane γ(C−H) bending mode of the C−H bonds attached at the end α-positions of the CPDT moiety. The methylene stretching and scissoring bands in the hexyl chains are even weaker in the polymer, which points to an improved parallel disposition of the CPDT plane to the gold surface, promoted by coupling.

3.3. Raman Analysis. *UV−vis Spectroscopy.* As a preliminary step to Raman analysis we report the optical characteristics of the investigated materials, of crucial importance for Raman excitation.

The UV−vis spectrum of the He_2CPDT-Au nanoparticle solution in toluene (Figure 3) exhibits the gold SP band at 530 nm, i.e., with no redshift compared with free AuNPs. In fact, no significant coupling of the SP with the π-system of the dithiophene occurs because the alkyl spacer is long. The presence of the CPDT moiety on the cluster surface is signaled by a band at 320 nm, as for the monomer in solution. Oligomers produced by coupling of He_2CPDTSH display a band at λ_{max} = 545 nm, which clearly overlaps the gold SP band in the polymeric cluster.

SERS. Surface-enhanced Raman scattering (SERS) has revolutionized the vibrational spectroscopy at surfaces and interfaces. The origin of the enhancement of Raman intensities (scattering cross-sections) at rough metal surfaces or metal nanoparticles is attributed to the contribution of two mechanisms: an electromagnetic (EM) enhancement and a chemical effect. Depending on the active substrate used and the nature of the molecular system to be studied, each of the two enhancement mechanisms can have dramatically different significance. For physisorbed randomly oriented molecules, the EM is the dominant mechanism and the interpretation of the SERS spectra is, in most cases, straightforward provided the reference molecule Raman spectrum is available. When the molecules are chemically adsorbed to the surface, bonding perturbs the electronic and vibrational structure of the adsorbate and the formation of the surface complex causes significant deviation from the reference Raman spectrum. In the latter cases, the observed SERS spectra of the surface complex is determined by fundamental vibrational modes of the complex (the chemisorbed molecule) and the constraints imposed by the molecular orientation and electric field polarization at the surface (surface selection rules).

He_2CPDTSH. The Raman spectrum of He_2CPDTSH is displayed in Figure 4a, whereas the sketched eigenvectors associated with the most important bands are given in Figure S4 of the Supporting Information. In the high-energy region, the spectrum shows two weak bands at about 3100 cm^{-1}, assignable to the aromatic stretching modes and several well resolved peaks below 3000 cm^{-1} corresponding to the aliphatic C−H stretching bands. Importantly, the peak at 2570 cm^{-1} must be assigned, according to DFT calculations, to the S−H stretching mode of the molecule.

The region below 1500 cm^{-1} is dominated by several modes at 1430, 1375, 1322, and 1080 cm^{-1}. In view of the DFT calculated eigenvectors, the peak at 1430 cm^{-1} is due to the C═C stretching of the aromatic oligothiophene ring. The bands at 1375 and 1322 cm^{-1} are assigned to CH_3 and CH_2 bending

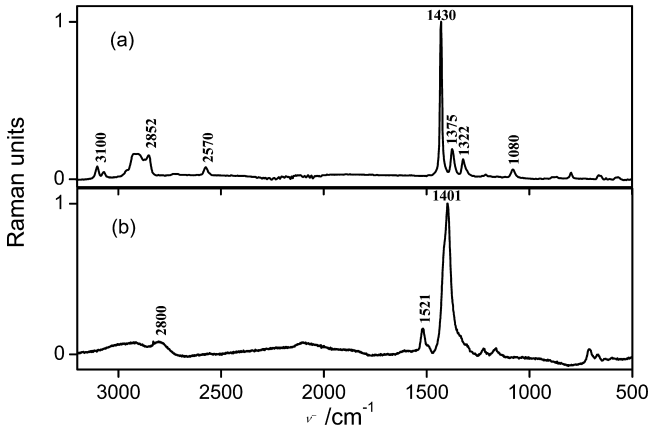

Figure 4. Raman spectra of (a) He_2CPDTSH and (b) He_2CPDT-Au (at 532 nm excitation).

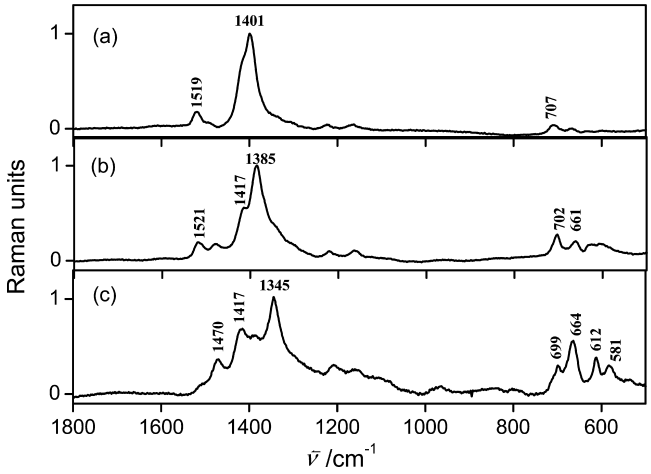

Figure 5. Raman spectra of He_2CPDT-Au at (a) 532, (b) 633, and (c) 785 nm excitation.

vibrations, and the 1080 cm^{-1} peak is due to the C−C stretching of the aliphatic chain.

He_2CPDT-Au Nanoparticles. The Raman spectra of He_2CPDT-Au nanoparticles were recorded with three laser lines, i.e., at 532, 633, and 785 nm (Figure 5). The Raman spectrum of He_2CPDT-Au (Figure 4b) is substantially different from that of He_2CPDTSH (Figure 4a). Differences in relative intensities and wavenumbers can only be explained in terms of chemical interaction between the oligomer and the gold nanoparticle. Most prominently, the bands near 2560 and 910 cm^{-1}, assigned to the S−H stretching and bending modes, respectively, as in the SEIRA spectrum, can no longer be detected. This is indicative of surface immobilization via sulfide bonding.

However, a close examination of the SERS spectra of He_2CPDT-Au (Figure 5) reveals that the characteristic C═C aromatic stretching mode around 1400 cm^{-1} is the most intense band in the spectra. Such a ring stretching mode also shows the most dramatic wavenumber downshift. Therefore, it is reasonable to conclude that an additional interaction exists between the aromatic rings and the gold nanoparticles. An ionic character of the aromatic rings is reflected in the lowering of the frequency of the C═C aromatic stretching mode and is indicative of partial charge transfer between the oligothiophene rings and the gold nanoparticle. In this regard, it must be pointed out that in going from neutral to oxidized or reduced species, the oligomer backbone changes from a heteroaromatic to a heteroquinoid structure. Due to this process, the double C═C bonds are weakened and molecular vibrations with a large content of C═C stretching shift downward in respect to the neutral form.[20] In fact, we find that the C═C aromatic stretching vibration is largely downshifted, by about 30 cm^{-1}, relative to the reference molecule.

SERS is the result of a combination of several enhancement mechanisms and thus depends sensitively on the detailed interactions between the molecule and the metal nanoparticle. Obviously, the EM mechanism, which arises from the strong local field very close to the metal surface due to the excitation of the metal plasmons, is the predominant contribution to SERS. However, in addition to this mechanism there are also several mechanisms that depend on the coupling between the molecules and the metal surface. One of the best known is the resonant charge transfer (CT) mechanism that arises when the incident light of the source is in resonance with a metal−molecule excitation. Less known is a nonresonant chemical mechanism due to specific interactions between the molecule and the metal. Although these mechanisms are not independent of each other, probably the latter is responsible for the important and unusual changes in the Raman of He_2CPDT-Au nanoparticles.

Spectra recorded upon various laser excitation wavelengths (Figure 5) show that as the latter decreases, the line around 1400 cm^{-1} shifts appreciably to higher frequencies: from 1345 cm^{-1} (at 785 nm) through 1385 cm^{-1} (at 633 nm), with a weak shoulder near 1345 cm^{-1}, to 1401 cm^{-1} (at 532 nm). Moreover, this strongest feature at 1401 cm^{-1}, excitaton at 532 nm, presents an asymmetry to the right side which indicates a weak contribution of the feature near 1385 cm^{-1}. These significant shifts to higher frequencies have proved that if the conjugation length increases when going from a neutral to an ionic oligomer, the frequency of this mode in the Raman spectra progressively decreases and dispersion of molecules with excitation wavelength is thus observed.[21] On the other hand, we can see that the Raman feature near 1470 cm^{-1} decreases when the laser exitation varies from 785 to 532 nm, becoming almost undetectable (Figure 5). All these experimental results indicate that we have different interactions between the oligomer and the metal surface, with modulated π-electron charge transfer (likely due to different spatial dispositions of the CPDT moieties with respect to the gold metal surface). Consequently, there is an additional molecular resonance mechanism that arises from the incident light of the laser being resonant with a molecule−molecule excitation leading to resonance Raman scattering.

Finally, concerning the polymerized nanoparticles, the Raman spectral responses of polymerized He_2CPDT-Au films with changing the laser excitation wavelength are essentially the same as that of the monomer (Figure S5 of the Supporting Information). This implies that polymerization does not significantly modify the interactions between the oligomeric thiophene rings and the metal surface.

3.4. Gold−Thiophene Interactions. The literature reports significant results on gold−thiophene interactions. The formation of self-assembled monolayers (SAMs) of thiophene oligomers on Au(111) surfaces was revealed by FTIR.[22] Thiophene and terthiophene form well-ordered SAMs on Au(111) surfaces from ethanol solutions. Structure and binding conditions of thiophene SAMs formed on Au(111) were investigated by STM and XPS.[23,24] High-resolution electron energy loss spectroscopy (HREELS) of oligothiophene films on gold confirmed that gold substrates generate a molecular orientation close to perpendicular.[25] These measurements have clearly demonstrated that the sulfur headgroups in thiophene would chemically interact with gold in the self-assembly process.

SCHEME 2

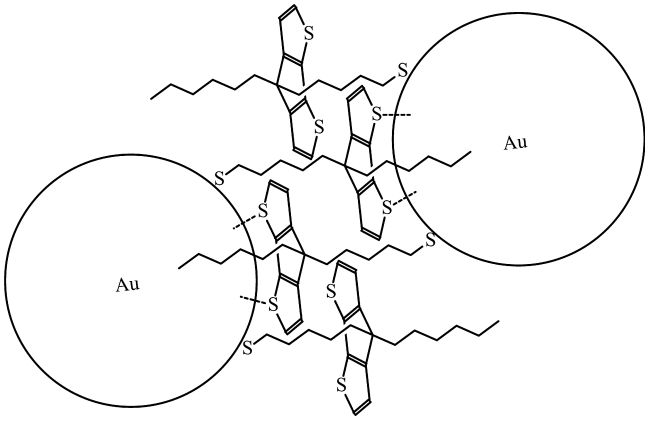

From these premises it is thus conceivable that the capped nanoparticles in close contact with each other show, at least partially, interpenetration of the organic chains (pictorially shown in Scheme 2), with frequent contacts between free gold surface sites and CPDT heads of caps. The formation of such links between the sulfur atoms of the CPDT moieties and gold may therefore be held responsible for the interaction detected in the Raman spectra.

4. Conclusions

Cyclopentadithiophene thiol and its polymer, connected via sulfide bridges with gold nanoparticles, have shown novel vibrational properties due to interactions of the thiophene moieties and the gold surface plasmons. The parallel disposition of the rigid oligothiophene chain in respect with the gold surface causes both a strong SEIRA effect, with surface enhancements of the IR response according to the infrared surface selection rule, and a SERS enhancement of the oligothiophene stretching band, assigned to coordination to the gold surface of neighboring particles via the thiophene sulfur atoms. This novel behavior may help to clarify the reciprocal interaction between oligothiophenes and gold nanoparticles, in light of their applications in electronic and optoelectronic devices.

Supporting Information Available: Calculated FT-IR spectrum and eigenvectors of He_2CPDTSH; Raman spectra of He_2CPDT-Au and poly(He_2CPDT-Au). This material is available free of charge via the Internet at http://pubs.acs.org.

References and Notes

(1) (a) Huynh, W. U.; Dittmer, J. J.; Alivisatos, A. P. *Science* **2002**, *295*, 2425. (b) Dabbousi, B. O.; Bawendi, M. G.; Onitsuka, O.; Rubner, M. F. *Appl. Phys. Lett.* **1995**, *66*, 1316. (c) Tseng, R. J.; Huang, J.; Ouyang, J.; Kaner, R. B.; Yang, Y. *Nano Lett.* **2005**, *5*, 1077.

(2) (a) Yeh, D. M.; Huang, C. F.; Chen, C. Y.; Lu, Y. C.; Yang, C. C. *Appl. Phys. Lett.* **2007**, *91*, 171103. (b) Kwon, M. K.; Kim, J. Y.; Kim, B. H.; Park, I. K.; Cho, C. Y.; Byeon, C. C.; Park, S. J. *Adv. Mater.* **2008**, *20*, 1253.

(3) Koller, D. M.; Hohenau, A,; Ditlbacher, H.; Galler, N.; Aussenegg, F. R.; Leitner, A; Krenn, J. R.; Eder, S.; Sax, S.; List, E. J. W. *Appl. Phys. Lett.* **2008**, *92*, 103304.

(4) Sih, B. C.; Wolf, M. O. *J. Phys.Chem. B* **2006**, *110*, 22298.

(5) Pucci, A.; Tirelli, N.; Willneff, E. A.; Schroeder, S. L. M.; Galembeck, F.; Ruggeri, G. *J. Mater. Chem.* **2004**, *14*, 3495.

(6) (a) Jeanmaire, D. L.; Van-Duyne, R. P. *J. Electroanal. Chem.* **1977**, *84*, 1. (b) Albrecht, M. G.; Creighton, J. A. *J. Am. Chem. Soc.* **1977**, *99*, 5215.

(7) Grabar, K. C.; Freeman, R. G.; Hommer, M. B.; Natan, M. J. *Anal. Chem.* **1995**, *67*, 735.

(8) (a) Chen, S. *Langmuir* **1999**, *15*, 7551. (b) Sarathy, V. K.; Narayan, K. S.; Kim, J.; White, J. O. *Chem. Phys. Lett.* **2000**, *318*, 543. (c) Youk, J. H.; Locklin, J.; Xia, C.; Park, M.-K.; Advincula, R. *Langmuir* **2001**, *17*, 4681. (d) Li, D.; Zhang, Y.; Li, J. *Microelectron. Eng.* **2003**, *66*, 91. (e) Sih, B. C.; Teichert, A.; Wolf, M. O. *Chem. Mater.* **2004**, *16*, 2712. (f) Wu, S.-H.; Huang, H.-M.; Chen, K.-C.; Hu, C.-W.; Hsu, C.-C.; Tsiang, R. C.-C. *Adv. Funct. Mater.* **2006**, *16*, 1959. (g) Anyaogu, K. C.; Cai, X. C.; Neckers, D. C. *Macromolecules* **2008**, *41*, 9000. (h) Zotti, G.; Vercelli, B.; Berlin, A. *Acc. Chem. Res.* **2008**, *41*, 1098. (i) Hong-Da, J.; Yen-Ching, T.; Sheng-Han, W.; Cheng-Hao, L.; Yu-Wei, S.; Raymond Chien-Chao., T. *J. Appl. Polym. Sci.* **2009**, *113*, 3972.

(9) (a) Zotti, G.; Vercelli, B.; Battagliarin, M.; Berlin, A.; Hernández, V.; López Navarrete, J. T. *J. Phys. Chem. C* **2007**, *111*, 5886. (b) Zotti, G.; Vercelli, B.; Berlin, A. *Chem. Mater.* **2008**, *20*, 397.

(10) Frisch, M. J.; Trucks, G. W.; Schlegel, H. B.; Scuseria, G. E.; Robb, M. A.; Cheeseman, J. R.; Montgomery, J. A., Jr.; Vreven, T.; Kudin, K. N.; Burant, J. C.; Millam, J. M.; Iyengar, S. S.; Tomasi, J.; Barone, V.; Mennucci, B.; Cossi, M.; Scalmani, G.; Rega, N.; Petersson, G. A.; Nakatsuji, H.; Hada, M.; Ehara, M.; Toyota, K.; Fukuda, R.; Hasegawa, J.; Ishida, M.; Nakajima, T.; Honda, Y.; Kitao, O.; Nakai, H.; Klene, M.; Li, X.; Knox, J. E.; Hratchian, H. P.; Cross, J. B.; Adamo, C.; Jaramillo, J.; Gomperts, R.; Stratmann, R. E.; Yazyev, O.; Austin, A. J.; Cammi, R.; Pomelli, C.; Ochterski, J. W.; Ayala, P. Y.; Morokuma, K.; Voth, G. A.; Salvador, P.; Dannenberg, J. J.; Zakrzewski, V. G.; Dapprich, S.; Daniels, A. D.; Strain, M. C.; Farkas, O.; Malick, D. K.; Rabuck, A. D.; Raghavachari, K.; Foresman, J. B.; Ortiz, J. V.; Cui, Q.; Baboul, A. G.; Clifford, S.; Cioslowski, J.; Stefanov, B. B.; Liu, G.; Liashenko, A.; Piskorz, P.; Komaromi, I.; Martin, R. L.; Fox, D. J.; Keith, T.; Al-Laham, M. A.; Peng, C. Y.; Nanayakkara, A.; Challacombe, M.; Gill, P. M. W.; Johnson, B.; Chen, W.; Wong, M. W.; Gonzalez, C.; Pople, J. A. Gaussian 03, Revision B.04; Gaussian Inc., Pittsburgh PA, 2003.

(11) Becke, A. D. *J. Chem. Phys.* **1993**, *98*, 1372.

(12) Stephens, P. J.; Devlin, F. J.; Chabalowski, F. C. F.; Frisch, M. J. *J. Phys. Chem.* **1994**, *98*, 11623.

(13) Scott, A. P.; Radom, L. *J. Phys. Chem.* **1996**, *100*, 16502.

(14) Francl, M. M.; Pietro, W. J.; Hehre, W. J.; Binkley, J. S.; Gordon, M. S.; Defrees, D. J.; Pople, J. A. *J. Chem. Phys.* **1982**, *77*, 3654.

(15) Hartstein, A.; Kirtley, J. R.; Tsang, J. C. *Phys. Rev. Lett.* **1980**, *45*, 201.

(16) Osawa, M. *Bull. Chem. Soc. Jpn.* **1997**, *70*, 2861.

(17) Osawa, M. *Topics Appl. Phys.* **2001**, *81*, 163.

(18) Hoffmann, F. M. *Surface Sci. Rep.* **1983**, *3*, 107.

(19) Osawa, M.; Ataka, K.; Yoshii, K.; Nishikawa, Y. *Appl. Spectrosc.* **1993**, *47*, 1497.

(20) Casado, J.; Hernández, V.; Hotta, S.; López Navarrete, J. T. *J. Chem. Phys.* **1998**, *109*, 10419. (b) Casado, J.; Hernández, V.; Hotta, S.; López Navarrete, J. T. *Adv. Mater.* **1998**, *10*, 1458.

(21) Hernández, V.; Ramírez, F. J.; Zotti, G.; López Navarrete, J. T. *J. Chem. Phys.* **1993**, *98*, 769.

(22) Matsuura, T.; Shimoyama, Y. *Eur. Phys. J.* **2002**, *E 7*, 233.

(23) Noh, J.; Ito, E.; Nakajima, K.; Kim, J.; Lee, H.; Hara, M. *J. Phys. Chem. B* **2002**, *106*, 7139.

(24) Dishner, M. H.; Hemminger, J. C.; Feher, F. J. *Langmuir* **1996**, *12*, 6176.

(25) Vilar, M. R.; Horowitz, G.; Lang, P.; Pellegrino, O.; do Rego, A. M. B. *Adv. Mater. Opt. Electron.* **1999**, *9*, 211.

JP1027355